Fire Technology

Imaging Through Fire Using Narrow-Spectrum Illumination

--Manuscript Draft--

Manuscript Number:	
Full Title:	Imaging Through Fire Using Narrow-Spectrum Illumination
Article Type:	Manuscript
Keywords:	Imaging; Fire; Narrow-spectrum illumination; Metrology; Blue light; Digital Image Correlation
Corresponding Author:	Matthew Stanton Hoehler, Ph.D. National Institute of Standards and Technology Gaithersburg, MD UNITED STATES
Corresponding Author Secondary Information:	
Corresponding Author's Institution:	National Institute of Standards and Technology
Corresponding Author's Secondary Institution:	
First Author:	Christopher M Smith, Ph.D.
First Author Secondary Information:	
Order of Authors:	Christopher M Smith, Ph.D.
	Matthew Stanton Hoehler, Ph.D.
Order of Authors Secondary Information:	
Funding Information:	
Abstract:	This paper demonstrates a simple method to enhance visibility through clean-burning flames that allows new opportunities to perform qualitative and quantitative optical metrology in fire research. The method combines narrow-spectrum, blue illumination and matched optical filters to reduce the influence of optical emissions from a glowing hot target and a large natural gas diffusion flame. The paper describes how the required illumination strength and filtering can be estimated from basic combustion and optical principles. Compared to white light, the required illumination to detect objects engulfed in flames with this method is reduced by a factor of 10^4. A series of experiments are conducted to determine the effectiveness of this method, successfully demonstrating the ability to take images of objects in natural gas fires up to 1000 kW using 200 W of illumination power.

Imaging Through Fire Using Narrow-Spectrum Illumination

Christopher M. Smith[1] and Matthew S. Hoehler[2]

[1] Berkshire Hathaway Specialty Insurance, 100 Federal Street, 20th Floor, Boston, MA, 02110, USA

[2] National Institute of Standards and Technology, 100 Bureau Drive, Gaithersburg, MD 20899, USA
(corresponding author: matthew.hoehler@nist.gov; ORCID: 0000-0002-6049-7560)

Imaging Through Fire Using Narrow-Spectrum Illumination

Abstract. This paper demonstrates a simple method to enhance visibility through clean-burning flames that allows new opportunities to perform qualitative and quantitative optical metrology in fire research. The method combines narrow-spectrum, blue illumination and matched optical filters to reduce the influence of optical emissions from a glowing hot target and a large natural gas diffusion flame. The paper describes how the required illumination strength and filtering can be estimated from basic combustion and optical principles. Compared to white light, the required illumination to detect objects engulfed in flames with this method is reduced by a factor of 10^4. A series of experiments are conducted to determine the effectiveness of this method, successfully demonstrating the ability to take images of objects in natural gas fires up to 1000 kW using 200 W of illumination power.

Acknowledgements

The authors would like to thank Behrang Hamadani for his assistance with the spectroradiometer measurements and Jeffrey Fagan for characterizing the filter transmittance spectra. We also thank Matthew Bundy, Laurean DeLauter and Anthony Chakalis at the National Fire Research Laboratory for their support in the execution of the fire experiments.

Keywords: Imaging, Fire, Narrow-spectrum illumination, Metrology, Blue light, Digital Image Correlation

1 Introduction

Imaging is a useful technique for observation and measurement in many fields of science and engineering, but is of particular importance for structural fire research. Tests of structural systems (buildings, bridges) involve many interacting components with failure mechanisms and locations that are often unknown prior to the start of an experiment. Real-time observation over large areas is critical to understanding the sequence and timing of failure. Historically, in large structural fire tests, experimentalists have had to rely on pre- and post-test surveys to characterize structural behavior [1, 2]. At ambient temperatures, quantitative optical metrology has become an increasingly popular tool for measurement in structural experiments. Techniques such as Digital Image Correlation (DIC) and Electronic Speckle Pattern Interferometry (ESPI) provide full-field strain and displacement measurements with higher accuracy and fewer physical constraints than traditional electromechanical sensors. The imaging of structural elements when fire is present, and thus the use of optical metrology, is currently hindered by several obstacles including the thermal radiation emitted from the fire and heated target, obscuration of the target by soot and smoke, and distortion of the images by light refraction in the heated air/smoke. While the burning of many types of combustible materials produces large quantities of soot and smoke that prohibit the use of some optical methods, most structural fire research can be conducted using clean-burning surrogate fuels like natural gas; leaving the radiation emitted by the flames and refraction-induced image distortion as the primary obstacles to imaging in a fire environment.

Successful imaging is based on detecting light reflected from a target object. This light, when reflected off a pattern or feature on the target surface, provides optical contrast which can be used for visualization and measurement. In the presence of fire, the reflected light reaching the image sensor may be much less intense than the emitted light from the flame, reducing the contrast and quality of the images. However, the emitted light from the flame is highly concentrated at the red end of the optical spectrum, and can be avoided by illuminating the target with shorter wavelength light.

This paper demonstrates the use of narrow-spectrum, blue (450 nm) illumination and matched optical filters to image in a structural fire testing environment. A steel plate (target) is suspended over a natural gas fire that is approximately 1-meter square at the base of the flames. Successful imaging results are demonstrated for fire sizes up to 1000 kW and target temperatures over 700 °C. Basic combustion and optics principles are applied to predict the relative intensity of the flame- and target-emitted radiation and the target-reflected illumination. These predictions are confirmed by the experiments.

2 Background

Thermal radiation presents a significant obstacle to imaging objects engulfed in fire (Figure 1). The radiation emitted by hydrocarbon fires can be divided into two main components. First, spectral emission bands are produced by the change in energy state of molecules during combustion. These spectral bands are mostly produced by carbon dioxide and water and result in emissions in the infrared range and therefore do not present significant challenges when imaging with visible light cameras[1]. The second source of thermal radiation from the fire is the black-body radiation emitted from suspended soot particles in the flames. Black-body radiation is emitted from solid matter, and the intensity and spectral content of the radiation are a function of temperature. Gas temperatures typical of combustion processes are between 1100 °C and 1700 °C, and in this range a significant fraction of the black-body radiation is emitted in the visible spectrum. A third, and less apparent, source of thermal radiation is emitted by hot objects, such as a structural member engulfed by a fire.

The intensity of thermal radiation emitted from a flame can be much higher than is typically used for imaging purposes. Heat fluxes of 100 kW/m^2 for a large diffusion flame is not uncommon. Most of this radiation is emitted in the infrared spectrum, but the basic principles and measurements that follow show

[1] Although radiation in the infrared spectrum is not a problem for the image quality, the imaging equipment (camera, lenses, cables) must be protected from the energy in this range; e.g. by shielding, appropriate filtering barriers, or placement at a sufficiently large distance from the fire to prevent damage.

that the intensity in the visible spectrum is on the order of 10 kW/m^2. In comparison, the typical irradiance of a brightly lit laboratory or office space is less than 0.01 kW/m^2 [3].

The visible portion of the flame emissions is a broad-band source and grows nearly exponentially with wavelength, such that the spectral intensity of the flame is 500 times greater for red light (750 nm) than for blue light (450 nm). If an imaging system (including applied filters) is sensitive only to relatively short visible wavelengths, the problem of seeing through flames becomes more tractable.

Grant [4] proposed the use of blue illumination and filters to compensate for target emissions of black-body radiation from a resistance-heated specimen; i.e. without flames. In his study, a random pattern was applied to the specimen by abrasion with silicon carbide paper and strains were measured up to 800 °C using Digital Image Correlation.

Pan [5] tested stainless steel plates heated to 1200 °C from the back side by an infrared heat source. The plates were illuminated with blue Light Emitting Diode (LED) lamps and a narrow-band filter was placed in front of the camera. The authors were successful at removing the effect of the emitted infrared radiation from the images and making measurements of the thermal strain in the plates.

Gales [6] applied a different, but related, solution to the problem of imaging targets in an environmental chamber. By providing sufficient broad-band illumination, narrow-band optical filters are not necessary. In his study, the maximum specimen temperature was 625 °C. Because the amount of radiation emitted from the surface grows as a function of temperature to the fourth power, this method becomes unpractical for significantly higher temperatures.

Cholewa [7] tested a composite plate specimen heated with a radiant panel to 500 °C. A novel application in that study was the simultaneous application of Digital Image Correlation and infrared thermography. The temperatures attained in that study were not sufficient to require specialized illumination sources.

McAllister [8] performed an exploratory study of Digital Image Correlation in an open flame environment. A steel plate was painted and instrumented with thermocouples, then suspended over a 70-kW fire produced by a natural gas burner. Due to the small size of the fire, minimal flame impingement on the target plate was observed and the specimens only reached temperatures of 200 °C.

As evidenced by the previous work described above, the use of narrow-spectrum illumination and filtering to enhance imaging in thermal environments is not new. However, with the exception of the work by Gales [6] and McAllister [8], past studies have dealt with the relatively small amount of thermal radiation emitted by hot objects, and not with the challenge posed by the more intense radiation emitted by a large fire. The study reported here was conducted to explore the possibility of using narrow-spectrum illumination and filtering to improve imaging in the large (structurally significant fires are on the order of megawatts), clean-burning fires utilized in structural fire research experiments.

3 Proposed Technique

The proposed technique builds on the work by Grant [4] and Pan [5] using narrow-spectrum illumination with a wavelength at the low end of the visible spectrum and spectrally-matched, band-pass optical filters. The past decade has seen significant advances in the availability of high-powered LEDs. LEDs are a naturally narrow-band light source whose wavelength is dependent on the diode chemistry. The second component in the imaging system is a band-pass or low-pass optical filter which blocks light of wavelengths higher than that emitted by the LED source. Combining a short-wavelength illumination source with an optical filter allows thermal radiation to be filtered out of the images. By using wavelengths in the visible part of the electromagnetic spectrum, common visible light cameras can be used for imaging.

Figure 2 shows a benchtop-scale demonstration of this technique. The distance from the camera to the target is about 1 m (Figure 2a). Figure 2b contains three images of the same small natural gas flame with different illumination and filtering methods applied. In the image on the left, no filters are used and the target is illuminated only by the ambient lighting in the room; the target is obscured by the flame. In the middle image, a 10 W 450 nm LED source is added to illuminate the target; improving the visibility of the target. In the image on the right, a band-pass optical filter is placed in front of the camera, blocking the light from the flame and allowing the target to be seen clearly.

4 Estimating Optical Power Requirements for Larger Fires

The problem of imaging a target through larger fires can be treated as an optimization of the signal-to-noise ratio. Successful imaging requires sufficient signal, in the form of optical energy reflected from the target, to overwhelm the ‘noise’ caused by the optical emissions of the flame. For large fires, it is not trivial to provide sufficient illumination to see through flames, and experimental considerations often preclude a trial-and-error approach. It is therefore useful to be able to estimate the optical power requirements beforehand.

This estimation will rely on a comparison of the amount of light produced by the flame and heated target, as well as the amount of light reflected by the illuminated target reaching the camera. The absolute measurements of these quantities are in terms of the energy hitting each camera pixel, which is dependent on the sensor size, resolution, and lens focal length. A more universally meaningful quantity to compare is the radiance (power per unit area per unit solid angle) of each of these sources. In the situation where the flame is co-located with the target, the radiance from each is proportional to the optical energy reaching the camera sensor.

4.1 Experimental setup

Figure 3 schematically illustrates the experimental setup and Figure 4 shows a photograph of the setup. The fire was produced by a 1 m × 1 m square natural gas diffusion burner. The burner was a stainless-steel sheet metal box with a 25-mm thick semi-permeable ceramic fiber lid to deliver an even gas supply to the entire burner area. A steel plate (305 mm × 305 mm × 6 mm) was suspended 0.75 m (to plate center) above the burner by a water-cooled support. The steel plate (target) was illuminated by two

100 W LED blue theater lights. This light source has a narrow beam angle (9 º) which allows the lights to be placed far from the fire, has a high-power level, and was manufactured with only blue LEDs. The lights were placed at roughly the same elevation as the target and located 3.5 m away and offset slightly (~ 0.75 m from centerline) to eliminate specular reflections that could cause unwanted bright spots in the images.

The blue LED lights were characterized experimentally at varying distances prior to the start of testing using a spectroradiometer with an integrating sphere detector. The intensity at the center of the light beam for a single light is predicted by the equation $I = (30\ W \cdot 15) \cdot D_{LED}{}^{-2}$, where I is the total irradiance directly in front of the light at distance D_{LED}, 30 W is the optical power emitted by the LED light (30 % efficiency for a 100 W light), and 15 is an empirical measure of the concentrating effect of the LED lens array. The intensity also varies with the distance from the center of the beam and is approximately normally distributed with respect to the offset angle, with a standard deviation of 4.4 degrees. The spectral distribution of the emitted light is nearly normally distributed (mean = 450 nm, standard deviation = 10 nm) as measured with the spectroradiometer[2].

A 5-megapixel charged-coupled device (CCD) camera (Allied Vision G-505B[3]) was located 3.5 m away from the target; on-center at the elevation of the plate. The camera was fitted with a 50 mm F2.8 C-mount Schneider Xenoplan lens with a locking focus and a series of two band-pass filters. The band-pass filters investigated are labeled Filter 1 (Midwest Optics BP470) and Filter 2 (Hoya B-440). The normalized quantum efficiency (QE) of the camera and the filter transmission spectra are shown in Figure 5. The filter transmission response was measured from 200 nm to 800 nm and it was assumed to reduce

---

[2] Users should be aware that high-intensity light in this frequency range can be harmful to your eyes. Appropriate eye protection and/or measures to prevent direct viewing of the light at close range are required.

[3] Certain commercial products are identified in this paper to specify the materials used and the procedures employed. In no case does such identification imply endorsement or recommendation by the National Institute of Standards and Technology, nor does it indicate that the products are necessarily the best available for the purpose.

linearly to zero at 10^5 nm. Two stacked filters were used because they provided a low-cost and effective band-pass filter at the desired frequency. Alternately, a single filter could be used.

We also placed a calibrated photodiode (Hamamatsu model S2281) with a visible spectral response and a calibrated heat flux gauge (Medtherm 64-1-20) in close proximity on the optical table aimed at the burner. The sensitivity of the photodiode was adjusted such that when the two sensors were exposed to the narrow-band 450 nm light source, they read the same value. However, when exposed to a natural gas fire the readings diverged; the heat flux gauge measured the entire radiative spectrum of the flame while the photodiode measured only the visible portion.

Previous studies have found that the target preparation and coating are a critical part of imaging targets at elevated temperatures [7, 8]. For tests of hot-rolled carbon steel, it is critical that the surface oxide layer (the 'mill scale') be removed before coating, as it naturally flakes off when heated above 400 ºC or when the steel yields. The mill scale was removed by sandblasting with a coarse abrasive (40/60 grit). A base layer of white high temperature spray paint was applied followed by a square grid stenciled in black spray paint to provide contrast (see Figure 4). The combination of a white base coat with a black pattern was found to be more temperature-resistant than the inverse. Due to the use of organic binders in most high-temperature paints, the manufacturers typically recommend curing the painted parts at high temperatures (>200 °C) to maximize the coating integrity. This curing step is infeasible for large structural elements, which may be difficult to place in a furnace and may develop unacceptable residual stresses or warping at these temperatures. A more moderate curing regime was used by heating the painted surface with a halogen lamp to 100 °C for 2 hours.

4.2 Radiance from flame

To characterized the radiance from the fire, we use the example of a fire with a constant heat release rate (HRR) of 800 kW produced by combustion of natural gas (~ 90 % methane). The radiative fraction (*RF*) was not measured directly, and is dependent on several factors including the combustion efficiency and specific fuel composition. Other researchers have found values for the radiative fraction for large natural gas flames which range from 0.15 to 0.4 [9, 10]. A value of 0.3 for the radiative fraction is assumed in the following calculations. These calculations assume a homogeneous volume for the radiative emissions, wherein the flames are optically thin. This is a simplification of the true behavior in which somewhat more emissions occur at and around the flame front, however it is supported by qualitative intensity observations of images of the flame.

Heskestad [11] provides an estimate for the mean flame height (H_f) in meters as:

$$H_f = -1.02 \cdot D + 0.235 \cdot \dot{Q}^{\frac{2}{5}} \qquad (1)$$

where D is the flame diameter at its base in meters and $\dot{Q}$ is the heat release rate in kilowatts. The time-averaged geometry of the flame is assumed to be a cone. Because we are using a 1-m square burner in this example, the effective diameter is taken as the diameter of an equivalent circular burner ($D = \frac{2}{\sqrt{\pi}} \cdot 1m = 1.13m$). For this diameter and an 800-kW fire, the Heskestad equation predicts a mean flame height of 2.25 m.

For an optical path at a height (h) above the burner surface, the optical path length (l) through the flame cone to the target is equal to:

$$l = \frac{D}{2} \cdot \left(1 - \frac{h}{H_f}\right) \qquad (2)$$

This is illustrated conceptually in Figure 6. For the current example, with h of 0.75 m the optical path length is 0.38 m.

To determine the optical radiation emitted by the flame along this path, consider a differential area (dA) of the flame as viewed by the camera. The relative volume (α_{rel}) of flame intersected by this region, compared to the volume of the entire flame cone is determined by:

$$\frac{l \cdot dA}{\left(\frac{\pi \cdot D^2 \cdot H_f}{12}\right)} = \alpha_{rel} \cdot dA \tag{3}$$

$$\alpha_{rel} = \frac{l}{\left(\frac{\pi \cdot D^2 \cdot H_f}{12}\right)} \tag{4}$$

where for the current example, this gives $\alpha_{rel} = 0.5\frac{1}{m^2}$.

The optical energy emitted from this portion of the flame is equal to the product of the total radiant energy and the relative volume. The radiance reaching the camera is determined by:

$$L_{flame} = \alpha_{rel} \cdot \dot{Q} \cdot \mathrm{RF} \cdot \frac{1}{\pi} \tag{5}$$

where the $1/\pi$ converts to steradians; considering the directional influence on hemispherical propagation of radiation. For the current example, this gives radiance from the flame of $38{,}224\,\frac{\mathrm{W}}{\mathrm{m}^2 \cdot sr}$.

4.3 Radiance from heated target

A second source of radiation that contributes to the ‘noise’ (unwanted signal) in an image is the radiation emitted from a glowing target; which is often present for structural materials in fires. Steel begins to glow red at about 460 °C but retains load carrying capacity until 700 °C [12]. Equation 6 describes the radiance of the target calculated per the Stefan-Boltzmann law for a grey-body:

$$L_{target} = \frac{\varepsilon \cdot \sigma \cdot T^4}{\pi} \tag{6}$$

Assuming an emissivity (ε) of the steel plate of 0.85 and using the Stefan-Boltzmann constant (σ) equal to $5.67x10^{-8}\frac{W}{m^2K^4}$; a target temperature ($T$) of 700 °C gives $L_{target} = 13{,}750\frac{\mathrm{W}}{\mathrm{m}^2\cdot sr}$.

4.4 Radiance from LED

The incident radiance to the target surface from the LED light source is described by Equation 7. This light is reflected from the matte painted target nearly evenly in all directions in the visible hemisphere. Typical values for the reflectivity (R) of 'white' paint ranges from 0.8 to 0.95 in the visible wavelengths, an intermediate value of 0.85 is assumed here. Thus, we can describe the reflected radiance from the white-painted surface as:

$$L_{LED} = (number\ of\ lights) \cdot \frac{450W}{{D_{LED}}^2} \cdot \mathrm{R} \cdot \frac{1}{\pi} \tag{7}$$

For two LED lights and $D_{LED} = 3.5\ m$, the reflected radiance is $20\frac{W}{m^2\cdot sr}$. Note that the value of 450 W only applies to the LED lights investigated here.

4.5 Spectral radiance visible to camera

The emitted radiance from the target and flames calculated in the previous sections are equal to the integrated value across all wavelengths. However, typical CCD sensors are sensitive mainly to visible wavelengths, so the emitted radiation from the flame must be reduced accordingly.

As described earlier, the light from the flame comes primarily from two sources: black-body radiation from heated soot (which includes emissions in the visible wavelengths) and spectral band emissions from the combustion products, principally CO_2 and H_2O (which are in the infrared and not visible to the camera). Determining the relative amount of black-body and spectral band radiation requires knowledge of the relative concentrations of soot and gas species. These fire parameters cannot be reliably estimated in typical structural test environments. As an alternative, the visible radiative fraction may be measured empirically for a specific fire. Figure 7 reports a series of measurements for the setup shown in Figure 4 made by the calibrated photodiode and heat flux gauge of a natural gas fire of monotonically increasing size. As indicated in the figure, the burner was ignited and the heat release rate was increased from 275 kW to 950 kW; the incident energy (irradiance) on the two sensors was recorded. As the heat flux and the incident visible radiative flux rise, the ratio between the two readings remains constant around a value of 0.360 ± 0.029 (expanded uncertainty). Therefore, the relative sensitivity can be used to estimate visible emissions from the flame independent of the fire size.

However, the photodiode is more sensitive to red and near-infrared light than the CCD array in the camera. Using the spectral sensitivities of the two sensors (photodiode and camera) and assuming a soot temperature, the relative intensity of light detected by the camera's CCD array was determined to be 0.078 times the total heat flux. The soot temperature of the flames (1390 °C) was estimated by comparing the black-body spectral radiance predicted by Planck's law with spectral radiance measured using the integrating sphere detector (Figure 8). Referring to the figure, the infrared portion of the spectrum is complicated by spectral emissions and obstructions, but the visible portion of the spectrum is predicted well by Planck's law.

Similar corrections were completed for the LED illumination reflected by the target and the grey-body radiation emitted from the target. Applying these corrections (camera sensitivities) to the results of Equations 5 to 7 determined the radiance detectable by the camera to have the following values: for the light emitted from the flame 2997 $\frac{W}{m^2 \cdot sr}$, for the light emitted from the hot target 0.56 $\frac{W}{m^2 \cdot sr}$, and for the LED illumination reflected by the target 16 $\frac{W}{m^2 \cdot sr}$. These values indicate (1) that the light emitted from the hot target that is detectable by the camera CCD array is insignificant compared to the light emitted from the flame, owing to the lower temperature of the target, and (2) that the total signal-to-noise ratio is approximately 1/190. This ratio supports the observation that it is not possible to detect contrast on the target with an unfiltered camera at this fire size. Figure 9 illustrates the various spectra resulting from these calculations. The plot shows the spectral radiance as a function of wavelength for the three sources of radiative emissions. The areas under each curve (integrated up to 10,000 nm) indicate the total radiance and are provided in the legend of the figure.

4.6 Application of band-pass filters

The band-pass filters are selected to significantly reduce the apparent brightness of the flame and target while minimizing the influence on the reflected LED illumination. Applying the measured transmission spectra of the filters (Figure 5) to Figure 9 yields the spectral radiance detected by the camera with both filters installed (Figure 10). Whereas in the previous figure the total LED illumination reflected from the target was much less than the emitted sources, in Figure 10 the situation is reversed. The reflected LED illumination (area under the curve) is nearly 2-times greater than that emitted by the flame, and more than 10^6 times greater than that emitted by the target.

5 Verification of Optical Power Requirements for Other Fire Sizes

In the example in the previous section, the signal-to-noise ratio improved from 0.0004 to 1.8 (a 10^4 improvement) for an 800-kW fire when the narrow-spectrum illumination and blue filters were added to the imaging system. Through that example, the sensitivity of the camera CCD array to the three sources of radiation (flames, target, LED) was empirically determined and scaling factors for the filter transmittances were established (Table 1). Note that the filter transmittance to the LED light only scales multiplicatively because the source is nearly monochromatic, whereas for the broad-band sources the full spectral response is necessary to model the filter combination.

Using the values in Table 1 the signal-to-noise ratios for other fire heat release rates can be predicted and compared with experimental observation. Figure 11 illustrates fire sizes for the investigated setup for a 200-kW fire with minimal flame impingement on the target plate and a 1000-kW fire where the target is fully engulfed in flames. The results are shown in Table 2 for fire sizes of 200 kW, 400 kW, 600 kW, 800 kW and 1000 kW. The following variables are held constant: distance between the target and the

LED (D_{LED}) is 3.5 m, the height of the target above the burner (h) is 0.75 m, and the target temperature (T) is always assumed to be 700 °C. Table 2 illustrates the improvement in signal-to-noise ratio across fire sizes and the limitations of the technique for larger fires.

Figure 12 shows two series of paired images captured by the Allied Vision G-505B camera for fire sizes ranging from 200 kW to 1000 kW in which the left-hand image uses narrow-spectrum lighting and filtering and the right-hand image does not. The left column in Figure 12 shows single images acquired by the camera. The improved visibility of the target when the lighting and filtering is used, in particular for smaller fire sizes, is illustrated. These experimental observations are a qualitative confirmation of the calculations summarized in Table 2. However, in an instantaneous sense the random turbulent nature of the large flame is not well represented by the geometric flame cone in Figure 6. Instead, the emission of thermal radiation is concentrated in hot spots within the flame, where it is more difficult to see the target than predicted. The turbulent heat gradients also pose a challenge in making quantitative measurements of the geometry of the target, as in DIC or ESPI. For these reasons it may be advantageous to record time-averaged composite images for visualization and analysis.

The right column in Figure 12 shows such composite images created from ten sequential frames (taken at 1 frame per second) at each fire size. By averaging the image over multiple frames, the transient effects of the flames are diminished, both in the view of the target and the apparent thermal distortion. The residual obstruction of the target in the left-hand images in Figure 12 is believed to be due to the soot in the flames. While increasing the LED lighting intensity or using filters with improved characteristics will allow users to see through larger fires, the soot present in larger and/or higher soot-yield fires is a limiting factor for using this technique.

6 Options to Further Improve the Technique

To further improve the optical power and signal-to-noise ratio for the narrow-spectrum illumination technique discussed in this paper, several options have been considered.

Pulsed illumination is a powerful method for improving the signal-to-noise ratio of optical signals [13]. By pulsing the light source on and off, one can in principle create images from which they can subtract a ‘dark frame’ (one with only the flame) from one with the flame and the narrow-spectrum illumination, resulting in an image which has only the illuminated target. A challenge for this approach is that the flame velocity is on the order of 0.1 m/s to 1 m/s. Subtracting the dark image from the illuminated image would require that the flame did not move between the two images, which would require a gap between the images of less than 1/100 to 1/1000 of a second. This requires specialized, and often expensive, cameras. The minimum signal-to-noise ratio achievable by this method is limited by the relative magnitude of the illumination and flame signal, and the bit depth of the camera sensors. Lock-in CCD cameras are available which perform this subtraction on a per-pixel basis before digitization, and are one option for extending this work to lower illumination levels.

Polarimetric imaging is based on measurement of the polarization state of light collected by a camera, and is a technique used for imaging through particulate and other visible obstructions [14]. One technique is to collect separate images of the vertically and horizontally polarized light, and subtract these channels. As the light scattered by airborne particulate or emitted by a flame is randomly polarized it will cancel out. Light reflected by a smooth surface, or produced by a polarized source, will be preferentially polarized in one direction and will stand out. Initial trials with this method by the authors were not successful due to the difficulty in preparing a surface coating which would withstand the fire without interfering with the polarization of reflected light. This problem would need to be addressed to apply this enhancement to the technique.

7 Conclusions

A simple method to enhance visibility through well-ventilated or clean-burning flames using narrow-spectrum illumination and matched optical filters is presented. It is shown how the improvement in signal-to-noise ratio can be estimated using basic combustion and optical principles. The approach is then applied experimentally to a series of natural gas burner fires ranging from 200 kW to 1000 kW. Compared to imaging using white light, the required illumination to detect a painted steel target engulfed in flames with this method was reduced by 10^4 for the investigated conditions. The technique provides significantly improved qualitative visual information in structural fire research and opens new possibilities to perform quantitative, image-based metrology in structural fire resistance experiments.

References

1. British Steel (1999) The behaviour of multi-storey steel framed buildings in fire. South Yorkshire, UK

2. Foster S, Chladná M, Hsieh C, et al (2007) Thermal and structural behaviour of a full-scale composite building subject to a severe compartment fire. Fire Saf J 42:183–199. doi: 10.1016/j.firesaf.2006.07.002

3. Shen E, Hu J, Patel M (2014) Energy and visual comfort analysis of lighting and daylight control strategies. Build Environ 78:155–170. doi: 10.1016/j.buildenv.2014.04.028

4. Grant BMB, Stone HJ, Withers PJ, Preuss M (2009) High-temperature strain field measurement using digital image correlation. J Strain Anal Eng Des 44:263–271. doi: 10.1243/03093247JSA478

5. Pan B, Wu D, Wang Z, Xia Y (2011) High-temperature digital image correlation method for full-field deformation measurement at 1200 °C. Meas Sci Technol 22:15701. doi: 10.1088/0957-0233/22/1/015701

6. Gales JA, Bisby LA, Stratford T (2012) New parameters to describe high-temperature deformation of prestressing steel determined using digital image correlation. Struct Eng Int J Int Assoc Bridg Struct Eng 22:476–486. doi: 10.2749/101686612X13363929517730

7. Cholewa N, Summers PT, Feih S, et al (2016) A technique for coupled thermomechanical response measurement using infrared thermography and digital image correlation (TDIC). Exp Mech 56:145–164. doi: 10.1007/s11340-015-0086-1

8. McAllister T, Luecke W, Iadicola M, Bundy M (2012) Measurement of temperature, displacement, and strain in structural components subject to fire effects: concepts and candidate approaches. doi: 10.6028/NIST.TN.1768

9. Hostikka S, McGrattan KB, Hamins A (2002) Numerical modeling of pool fires using large eddy simulation and finite volume method for radiation. Fire Saf Sci -- Proc Seventh Int Symp M:383–394.

10. Beyler CL (2008) Fire hazard calculations for large open hydrocarbon fires. SFPE Handb. Fire Prot. Eng.

11. Heskestad G (1983) Luminous heights of turbulent diffusion flames. Fire Saf J 5:103–108. doi: 10.1016/0379-7112(83)90002-4

12. Seif M, Main J, Weigand J, et al (2016) Temperature-Dependent Material Modeling for Structural Steels: Formulation and Application. doi: 10.6028/NIST.TN.1907

13. Wolfson R (1991) The lock-in amplifier: A student experiment. Am J Phys 59:569–572. doi: 10.1119/1.16824

14. Chenault DB, Pezzaniti JL (2000) Polarization imaging through scattering media. In: Chenault DB, Duggin MJ, Egan WG, Goldstein DH (eds) Proc. SPIE. pp 124–133

15. Choe, L., Ramesh, S., Hoehler, M., Bundy, M., Seif, M., Zhang, C., Gross J (2017) National Fire Research Laboratory commissioning project: Testing steel beams under localized fire exposure (NIST TN 1977). Gaithersburg, MD

Tables

Table 1 Camera sensitivity and filter transmittance for the radiation sources

Source	Camera sensitivity, -	Transmittance, -		
		Filter 1	Filter 2	F1 + F2
Flame	0.078	0.0178	0.0053	0.0012
Hot Target	4.06E-05	0.0201	2.5E-05	2.6E-06
LED light	0.819	0.4265	0.905	0.386

Table 2 Emitted radiance and radiance visible to the camera CCD after filtering for various fire sizes

Heat Release Rate ($\dot{Q}$), kW	Flame height (H_f), m	Optical path length (l), m	α_{rel}, -	Emitted radiance, $W/(m^2*sr)$				Radiance visible after filtering, $W/(m^2*sr)$			
				Flame (L_{flame})	Target (L_{target})	LED (L_{LED})	SNR, -	Flame ($L_{flame,f}$)	Target ($L_{target,f}$)	LED ($L_{LED,f}$)	SNR_f, -
1000	2.57	0.40	0.47	44454	13750	20	0.0003	4.0	1.4E-06	6.3	1.6
800	2.25	0.38	0.50	38224	13750	20	0.0004	3.5	1.4E-06	6.3	1.8
600	1.88	0.34	0.54	30941	13750	20	0.0004	2.8	1.4E-06	6.3	2.2
400	1.43	0.27	0.56	21466	13750	20	0.0006	1.9	1.4E-06	6.3	3.2
200	0.80	0.04	0.14	2692	13750	20	0.0012	0.2	1.4E-06	6.3	25.8

Figures

Figure 1 Natural gas flames (700 kW) obstructing the view of a structural steel beam experiment [15]

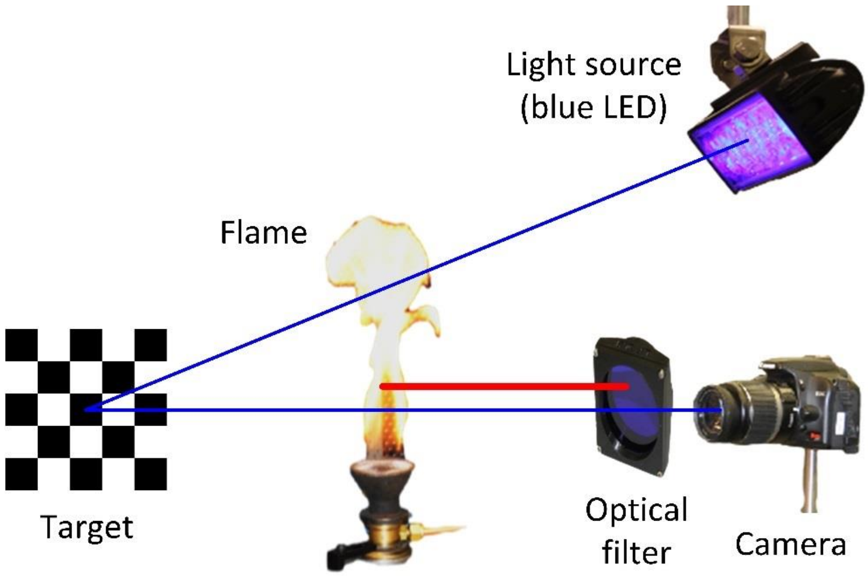

(a)

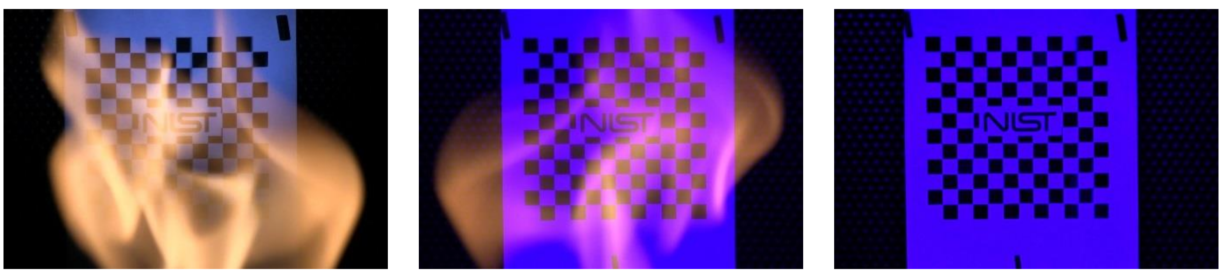

(bi) *(bii)* *(biii)*

Figure 2 Benchtop-scale demonstration of imaging technique: (a) illustration of setup (not to scale) and (b) target viewed through 5 kW natural gas flame when illuminated with i) ambient light, ii) 10 W of 450 nm light, and iii) 10 W of 450 nm light and imaged through a band-pass filter

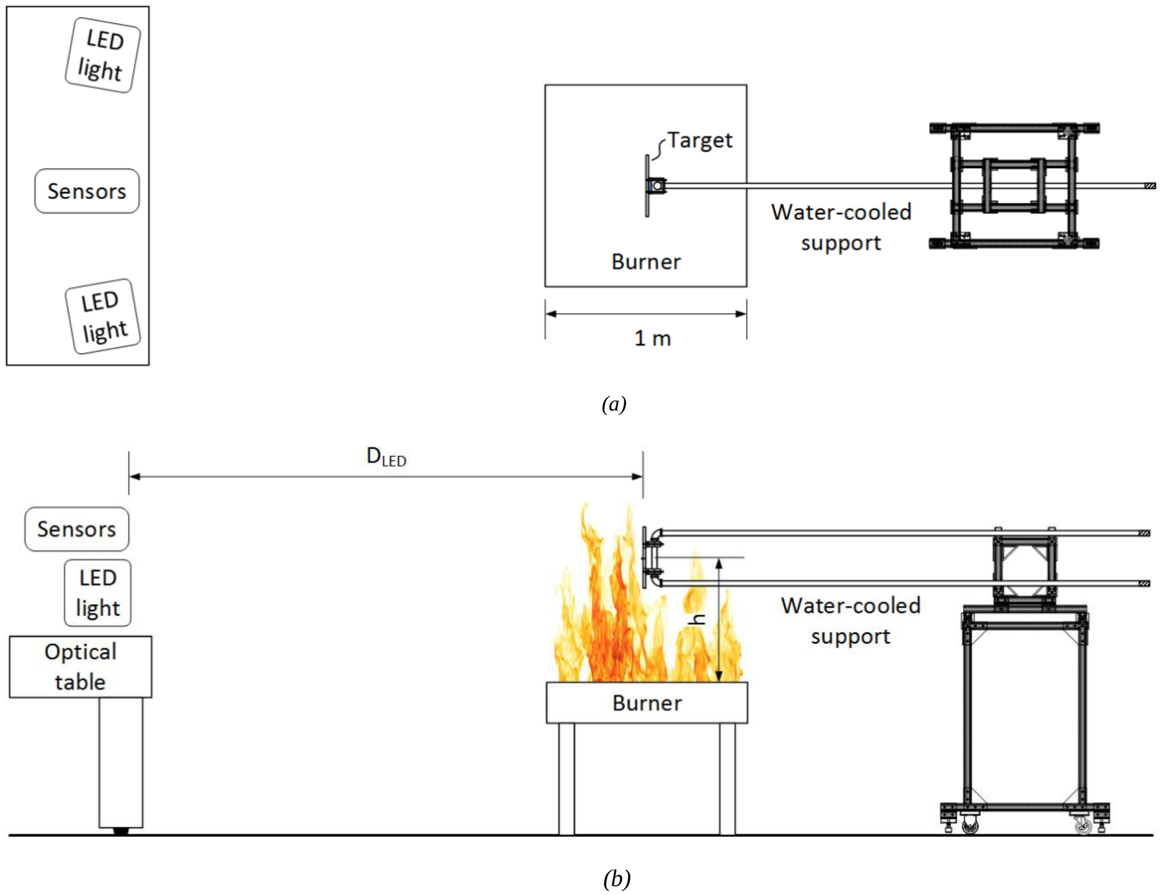

Figure 3 Schematic of setup for large-scale tests: (a) plan view and (b) elevation view

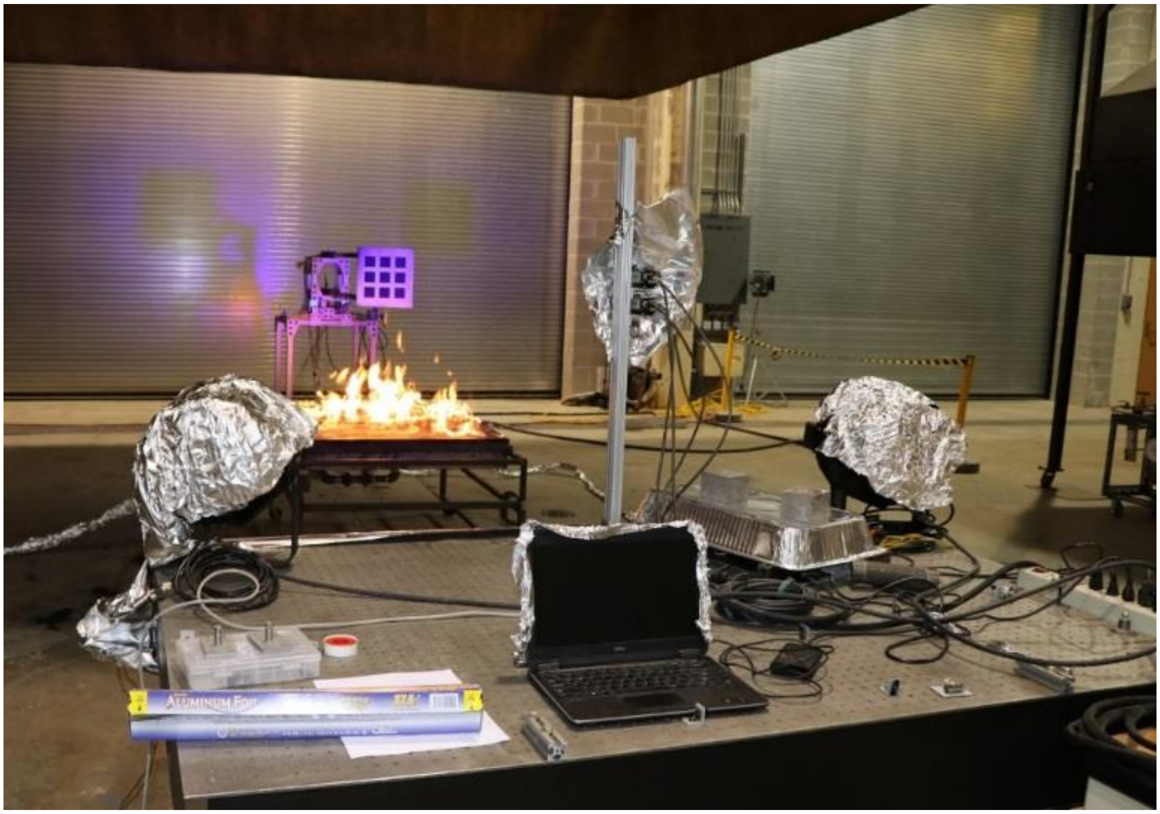

Figure 4 Photograph of setup for large-scale tests

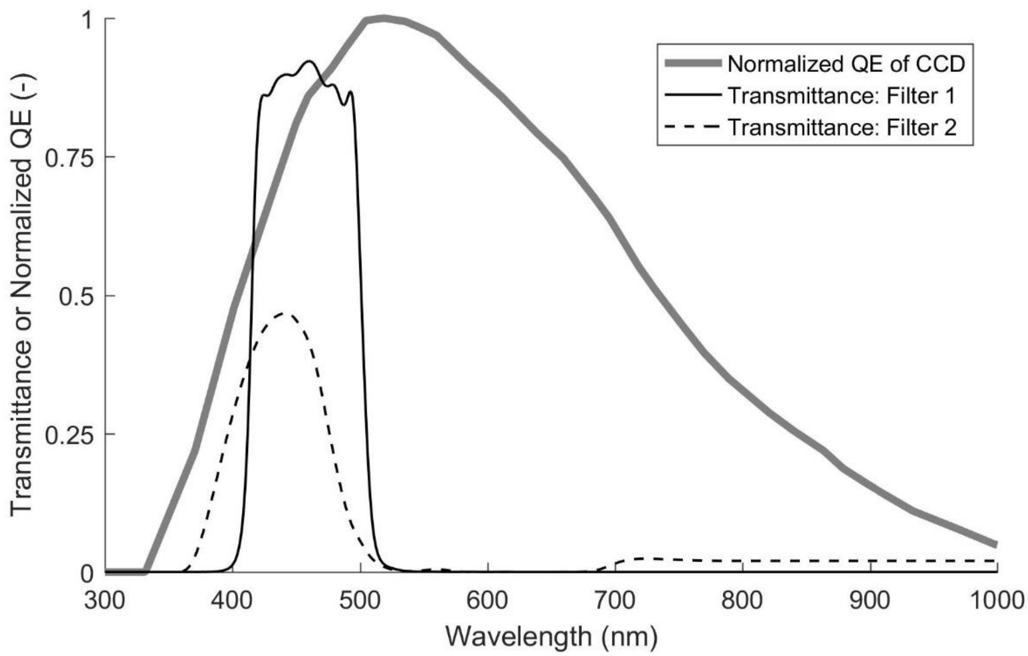

Figure 5 Spectral response of filters and camera CCD array (QE = Quantum efficiency)

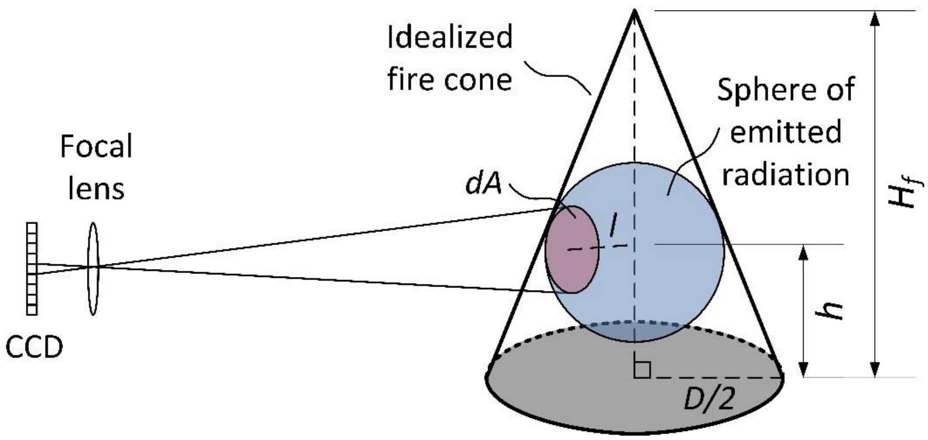

Figure 6 Conceptual illustration of radiation emitted from the flames as viewed by the camera

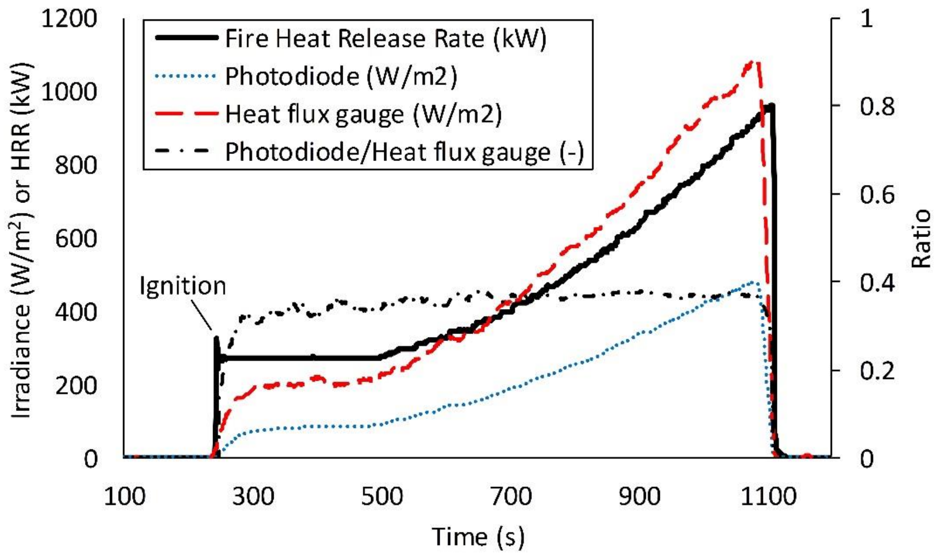

Figure 7 Measurements of incident energy 3.5 m from the target as a function of time for a monotonically increasing heat release rate (HRR) from 275 kW to 950 kW over 850 s

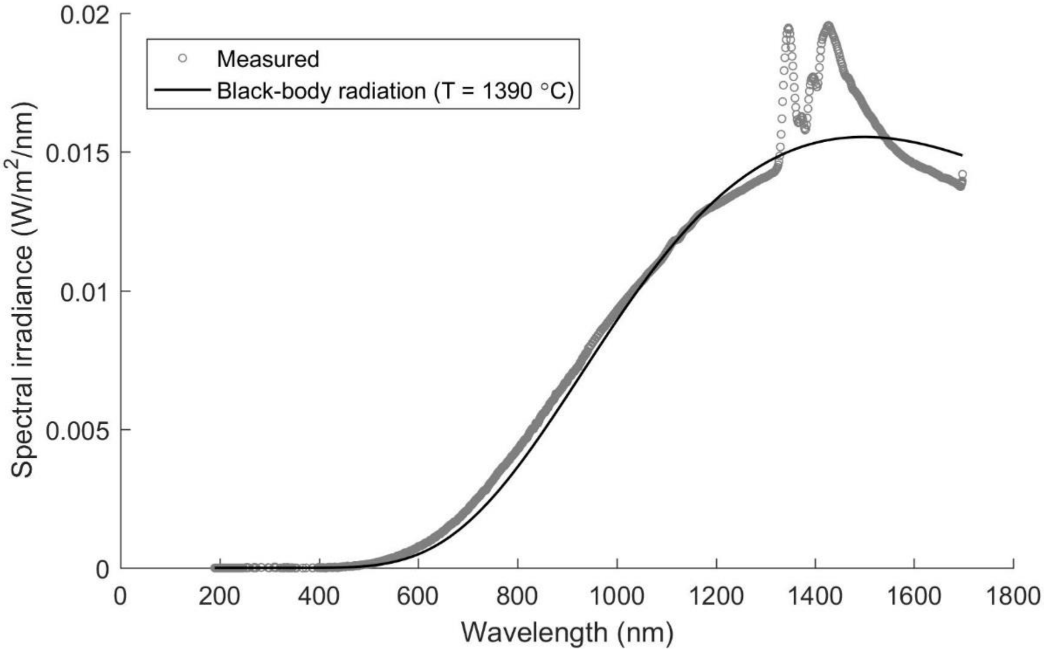

Figure 8 Comparison of measured and predicted spectral radiance between 200 nm and 1700 nm wavelengths

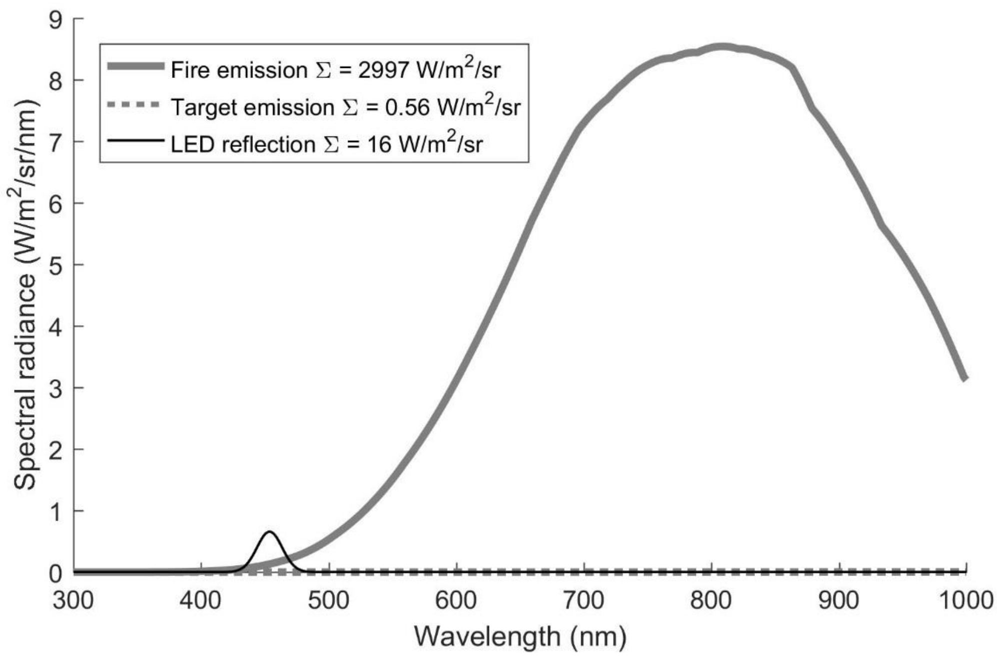

Figure 9 Spectral radiance of each source of emissions as visible with the CCD array

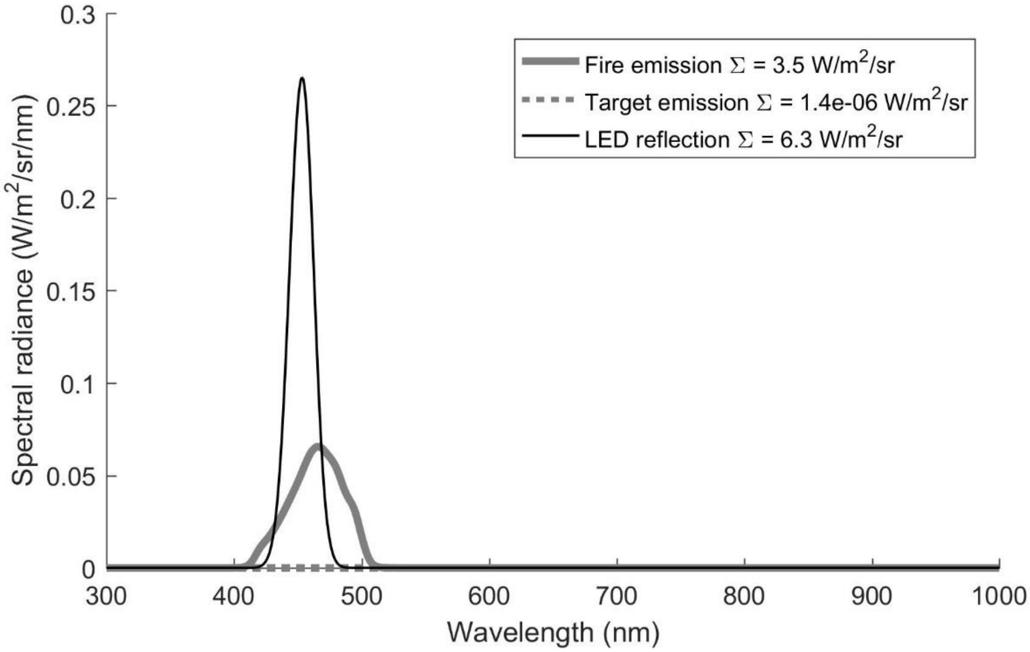

Figure 10 Spectral radiance of each source of emissions as visible with the CCD array with filters applied

(a) (b)

Figure 11 Photographs of varied fire sizes: (a) 200-kW fire and (b) 1000-kW fire

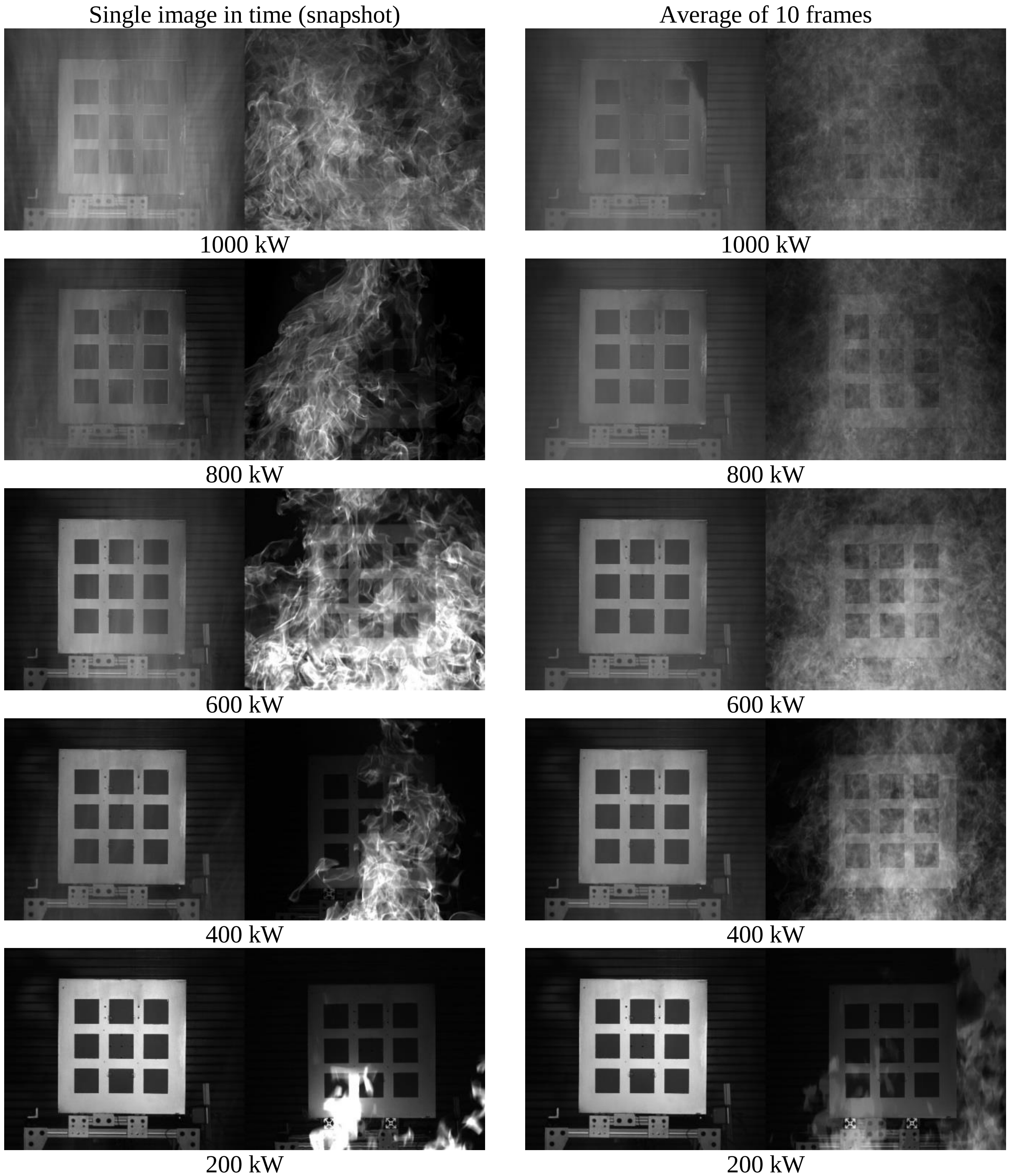

Figure 12 Paired images in which the left-hand image uses narrow-spectrum lighting and filtering and the right-hand image does not. The column of paired images on the left is for a single snapshot in time, whereas the column of images on the right is the average generated from 10 consecutive frames